

# Elastic aging from coexistence and transformations of ferroelectric and antiferroelectric states in PZT

F. Cordero\* and F. Craciun

CNR-ISC, Istituto dei Sistemi Complessi, Area della Ricerca di Roma - Tor Vergata,  
Via del Fosso del Cavaliere 100, I-00133 Roma, Italy

F. Trequattrini

Dipartimento di Fisica, Università di Roma "La Sapienza",  
P.le A. Moro 2, I-00185 Roma, Italy and CNR-ISC

P. Galizia and C. Galassi

CNR-ISTEC, Istituto di Scienza e Tecnologia dei Materiali Ceramici, Via Granarolo 64, I-48018 Faenza, Italy

(Dated: August 28, 2018)

Materials undergoing antiferroelectric/ferroelectric (AFE/FE) transitions are studied for possible applications that exploit the large volume, charge and entropy differences between the two states, such as electrocaloric cooling, energy storage, electromechanical actuators. Though certain compositions of  $\text{PbZr}_{1-x}\text{Ti}_x\text{O}_3$  (PZT) codoped with La and Sn may withstand millions of electrically induced AFE/FE cycles, in other cases few thermally induced cycles and room temperature aging may cause noticeable changes in the material properties. This is particularly evident in the elastic moduli, which at room temperature can become as much as four times softer. In order to get more insight into the mechanisms involved in such elastic aging and full recovering with mild annealing at 600 – 800 K, the effect of La doping on  $\text{PbZr}_{0.954}\text{Ti}_{0.046}\text{O}_3$  is studied with anelastic measurements. Complete suppression of the time dependent phenomena is found after the transformation of the intermediate FE phase into incommensurate AFE by 2% La doping. This is discussed in terms of disappearance of the stress and electric fields at the FE/AFE interfaces, in the light of the thermally activated anelastic relaxation processes that are observed at high temperature, and are due to mobile defects, presumably O vacancies.

## I. INTRODUCTION

Among the antiferroelectric materials,  $\text{PbZrO}_3$ -based perovskites have been intensively investigated due to their electrically induced antiferroelectric/ferroelectric (AFE/FE) transition, which is generally accompanied by large changes in volume and charge<sup>1</sup>. These properties are very appealing for potential use in various applications such as strain actuators, high energy storage capacitors, pulsed power generators, *etc*<sup>1,2</sup>. Various doping strategies have been employed to tailor the phase transformation behavior of  $\text{PbZrO}_3$ -based materials in order to improve their performances. Thus, the most widely used dopants to reduce the critical field are  $\text{La}^{3+}$ ,  $\text{Ba}^{2+}$ ,  $\text{Ca}^{2+}$  on the  $\text{Pb}^{2+}$  site and  $\text{Sn}^{4+}$ ,  $\text{Ti}^{4+}$  and  $\text{Nb}^{5+}$  on the  $\text{Zr}^{4+}$  site<sup>1,3</sup>. The AFE/FE transition in  $\text{PbZrO}_3$ -based perovskites is also associated with high entropy changes and electrocaloric/pyroelectric effects, which are very interesting for novel applications such as solid state cooling and pyroelectric energy harvesting<sup>4-7</sup>. For example, in  $\text{Pb}_{0.97}\text{La}_{0.02}(\text{Zr}_{0.95}\text{Ti}_{0.05})\text{O}_3$  a maximum reversible adiabatic temperature change of 8.5 °C has been obtained near the phase transition temperature together with a very large recoverable energy density of 12.4 J/cm<sup>3</sup> at room temperature<sup>5</sup>. Materials that are both AFE and FE and show electrocaloric effect and devices based on them have been recently reviewed in Refs. 6–8, and their readiness for use in heat pumping applications has been pointed out. Actually solid-state cooling devices, includ-

ing those based on the electrocaloric effect, are among the priorities in various national and international energy programs, as listed *e.g.* in Refs. 6 and 7. However, major challenges for introducing ferroic materials in practical cooling applications are still unsolved. Since electrocaloric cooling uses the entropy changes associated with first order phase transformations, structural changes and fatigue under repetitive electrical stress are important issues<sup>6</sup>. Cycle stability and fatigue are also fundamental issues for electromechanical actuators. Both refrigeration devices and strain actuators must withstand a huge number of cycles during their lifetime, and therefore understanding effects like creep and fatigue, occurring at longer functioning time scale, is mandatory for practical applications.

Previous works showed that the formation of the AFE phase in undoped and doped  $\text{PbZrO}_3$  may be slow and accompanied by aging phenomena, and it has been proposed that this is due to extended defects forming at the FE/AFE interfaces in order to accommodate the large volume difference between the AFE and FE phases<sup>9</sup>. Aging and thermal cycling through the AFE/FE transition may also cause outstanding softenings of the Young's modulus and splitting of the antipolar and octahedral tilt modes involved in the AFE/FE transition, which however can be fully recovered with mild annealing<sup>10,11,12</sup>. In order to better understand the nature of these phenomena in  $\text{PbZrO}_3$ -based materials, and in particular whether the orthorhombic AFE phase itself plays a particular role, we

study here the effect of La doping on the elastic aging. Doping with La destabilizes the FE phase at the expenses of the AFE, and above 1% La changes the intermediate FE phase into incommensurate (IC) AFE<sup>13,14</sup>. Such a change completely suppresses the irreversible softenings, that occur during aging and temperature cycling, indicating that they are indeed due to the coexistence of the AFE and FE phases.

## II. EXPERIMENTAL

Ceramic samples of  $\text{PbZr}_{0.954}\text{Ti}_{0.046}\text{O}_3$  (PZT 95.4/4.6 or PZT) and  $\text{Pb}_{0.97}\text{La}_{0.02}\text{Zr}_{0.954}\text{Ti}_{0.046}\text{O}_3$  (PLZT 2/95.4/4.6 or PLZT) were prepared by the mixed-oxide method in the same manner as previous series of samples<sup>15,16</sup>. The oxide powders were calcined at 800 °C for 4 hours, pressed into bars for the anelastic and into pellets for the dielectric experiments, sintered at 1250 °C for 2 h and packed with  $\text{PbZrO}_3 + 5\text{wt}\%$  excess  $\text{ZrO}_2$  to prevent PbO loss. The powder X-ray diffraction did not reveal any trace of impurity phases. The densities were about 95% of the theoretical values and the grains were large, with sizes of 5 – 20  $\mu\text{m}$ . Diffractograms were also measured around the AFE/FE transition and fitted with the Rietveld method, in order to extract the pseudocubic cell volumes of the coexisting O-AFE (*Pbam* space group<sup>17</sup>), IC-AFE (no space group is reported for this phase and we used *Pnmm*<sup>18</sup>) and R-FE phases (*R3m* space group<sup>19</sup>).

For the anelastic experiments bars were cut 0.6 mm thick and up to 4 cm long and Ag paint electrodes were applied to the bars and pellets. The dielectric permittivity  $\varepsilon = \varepsilon' - i\varepsilon''$ , with losses  $\tan\delta = \varepsilon''/\varepsilon'$ , was measured with a HP 4284A LCR meter with a four-wire probe and an electric field of 0.5 V/mm, between 0.2 and 200 kHz, controlling temperature with a modified Linkam HFS600E-PB4 stage. The dynamic Young's modulus  $E = E' - iE''$ , was measured by suspending the bars on thin thermocouple wires in vacuum and electrostatically exciting their flexural modes<sup>20</sup>. The data are presented as compliance  $s = 1/E = s' - is''$ , normalized to the stiffer value  $s_0$  in the PE phase, with losses  $Q^{-1} = s''/s'$ . The real part was deduced from the resonance frequency  $f \propto \sqrt{E'}^{21}$ , as  $s(T)/s_0 \simeq f_0^2/f^2(T)$ , with  $f_0 = 1 - 5$  kHz for the fundamental mode, depending on the sample composition and length.

## III. RESULTS

Figure 1 shows the real parts and losses of the dielectric permittivity  $\varepsilon$  (red) and elastic compliance  $s$  (blue) of PZT 95.4/4.6, measured at 1 kHz and  $\sim 1.9$  kHz respectively, during heating (open symbols) and cooling (closed symbols). When cooling through  $T_C$  from the cubic (C) paraelectric (PE) to the rhombohedral (R) FE phase, there is a drop of  $\varepsilon'$  and positive jump of  $s'$ . The

jump in  $\varepsilon'$  is due to the first order nature of the transition, though the thermal hysteresis is only 2.5 K. Notice the logarithmic scale of  $\varepsilon'$  in order to put in evidence the anomalies at the AFE transitions.

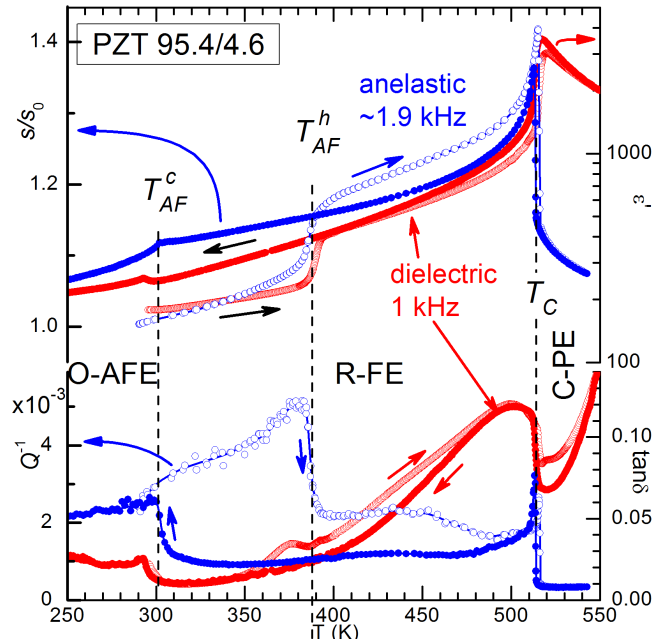


FIG. 1. Real parts (upper panel) and losses (lower panel) of the elastic compliance and dielectric susceptibility of PZT 95.4/4.6.

The transition between the R-FE and the orthorhombic (O) AFE phase has a large thermal hysteresis, and the susceptibility curves during cooling may strongly depend on the cooling rate and state of the sample<sup>10,11</sup>. For this reason, the two temperatures  $T_{AF}^c$  from the  $s$  and  $\varepsilon$  curves are different, and the anomaly in  $\varepsilon'$  has not the same shape as during heating. Instead, the reverse transition during heating occurs always at the same temperature  $T_{AF}^h$  accompanied by a steplike increase of the susceptibilities.

Figure 2 shows the evolution of the compliance of another sample of PLZT 95.4/4.6 during thermal cycles and aging at room temperature for overall one month. The sample of Fig. 1 also presents similar behavior, but was subjected to a smaller number of cycles and for a shorter time. The anomaly of  $s'$  at  $T_{AF}^h$  in Fig. 1 differs from those in Fig. 2 for the lack of a spike, which appeared in the fourth cycle (not shown). The shape of the elastic anomaly at  $T_{AF}$  depends on the sample and its history and can be fitted with the superposition of two steps of opposite signs corresponding to the transitions in the polar and octahedral tilt modes; apparently, the transition kinetics of these modes may be differently affected by aging and fatigue, resulting in a variety of shapes<sup>10,11</sup>. The spike arises from a slight shift in  $T$  of the centers of the two opposite steps. As described for similar compositions around 5% Ti<sup>10,11</sup>, there is a progressive softening

associated both with aging at room temperature, in a state of coexisting AFE and FE phases, and with cycling through the temperature driven AFE/FE transitions. In the sample of Fig. 2 the compliance exhibits an impressive softening of nearly four times at room temperature with respect to the stiffer state just after a final high temperature annealing. Not all the measured  $s'$  curves are displayed for clarity; the numbers count the cycles that include runs through  $T_{AF}^h$  and sometimes  $T_C$ , without exceeding it too much. In fact, when heated above 600 K, the sample starts recovering the original stiffness and shape of the anomaly at  $T_{AF}$ , as shown by cycles 5 and 6. The latter was extended up to 850 K, causing so complete an anneal, that the stiffness subsequently reached at room temperature was even higher than at the starting point, where some aging had already occurred. Notice that no reoxygenation of excess O vacancies was possible during the high temperature cycles, because they were made in a vacuum better than  $10^{-5}$  mbar and at a fast rate, 5 – 6 K/min above 600 K.

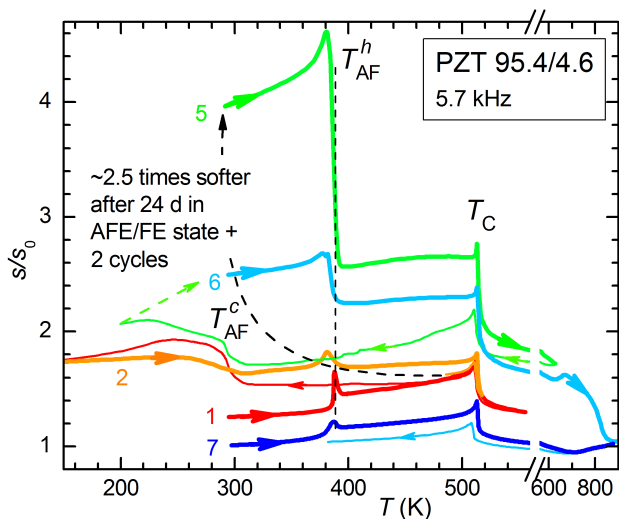


FIG. 2. Evolution of the compliance of PZT 95.4/4.6 during aging at room temperature and the thermal cycles numbered in the labels.

Similar tests have been conducted on PLZT 2/95.4/4.6. The anelastic and dielectric curves in the virgin state are shown in Fig. 3. A major difference with the undoped composition is a closer correspondence between the  $\epsilon$  curves during cooling and heating, with reduced thermal hysteresis  $T_{AF}^h - T_{AF}^c$ , indicating a faster kinetics and no complications of splitting of antiferrodistortive and polar modes below  $T_{AF}$ . In addition, the elastic response of the intermediate phase between  $T_{AF}$  and  $T_C$  has changed, as put in evidence in Fig. 4; here the  $s'$  heating curves of undoped and La doped PZT are compared and the dashed region corresponds to the piezoelectric softening<sup>22</sup> within the FE phase of PZT, totally absent in PLZT, so that even the sign of the step at  $T_{AF}$  has changed.

The disappearance of the piezoelectric softening with

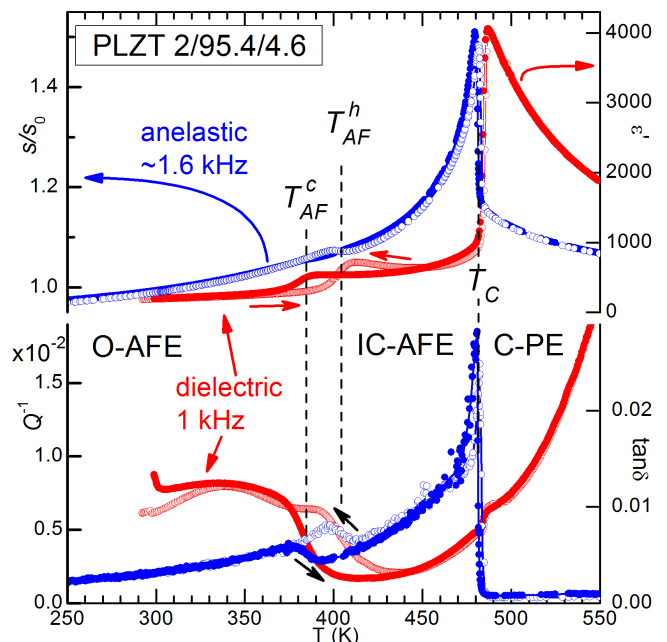


FIG. 3. Real parts (upper panel) and losses (lower panel) of the elastic compliance and dielectric susceptibility of PLZT 2/95.4/4.6.

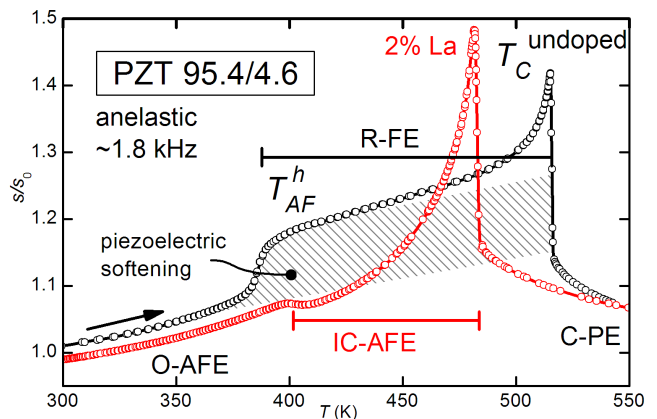


FIG. 4. Comparison of the compliances of PZT 95.4/4.6, undoped and doped with 2% La, measured during heating.

2% La doping is in agreement with the PLZT  $x/95/5$  phase diagram<sup>13,14</sup>, according to which for  $x(\text{La}) > 0.01$  the intermediate R-FE phase becomes IC-AFE. Sections of the  $x(\text{La}) - y(\text{Ti}) - T$  phase diagram of PLZT are shown in Fig. 5, together with the transition temperatures of the present samples.

The La-doped composition has a completely different behavior under aging at room temperature and thermal cycling with respect to the undoped case, as shown in Fig. 6.

In contrast with PZT, PLZT remains remarkably constant over time and cycles: the room temperature compliance remains within  $\pm 0.3\%$  of the starting value during 9

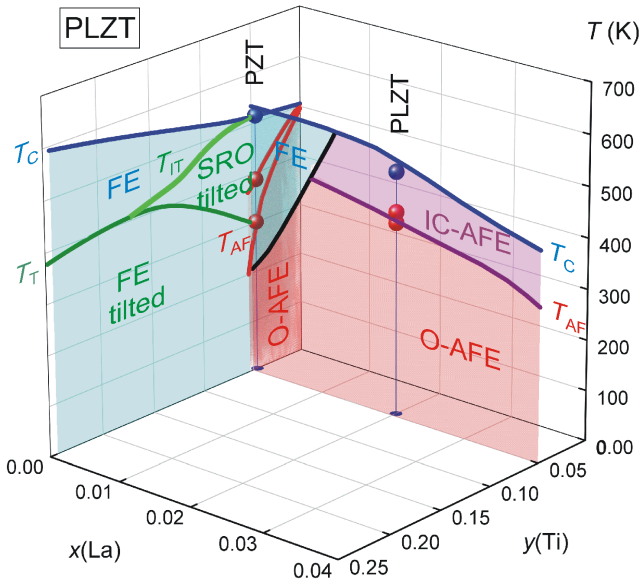


FIG. 5. Sections  $x(\text{La}) = 0^{23}$  and  $y(\text{Ti}) = 0.05^{14}$  of the phase diagram of PLZT. The points are the transitions temperatures of the samples tested here.

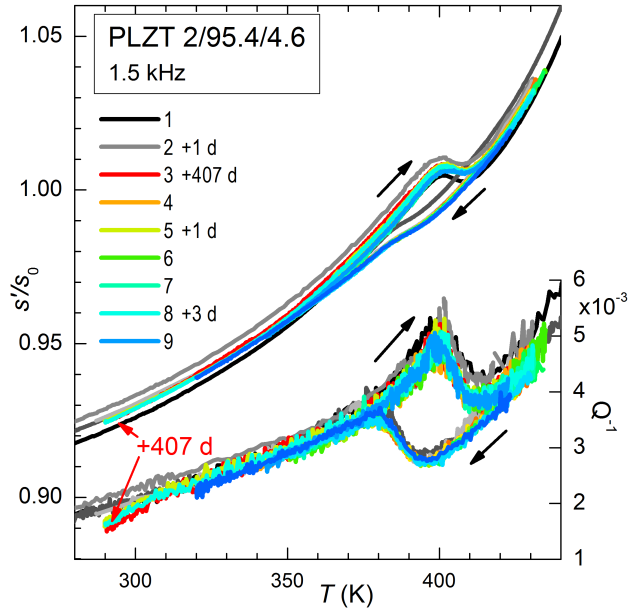


FIG. 6. Evolution of the compliance of PLZT 2/95.4/4.6 during aging at room temperature in the AFE state and thermal cycles.

cycles, one of which extended to 760 K, distributed over 410 days, and the  $s'$  and  $Q^{-1}$  steps at  $T_{AF}$  are exactly reproducible. In addition, the amplitude of the  $s'$  step is greatly reduced with respect to PZT.

#### IV. DISCUSSION

The ion  $\text{La}^{3+}$  in coordination 12 has a radius of 136 pm, instead of the 149 pm of  $\text{Pb}^{2+}$ , and the consequent reduction of the cell volume is likely an important factor in the stabilization of the AFE phase, that has a smaller volume than the FE one<sup>24</sup>. This is confirmed by the volumes of the pseudocubic cells deduced from Rietveld refinements of the x-ray diffractograms taken around  $T_{AF}$  and reported in Fig. 7. There is a more than tenfold decrease of the volume misfit between the O-AFE and R-FE cells in PZT from  $(0.6 \pm 0.07)\%$  to  $(-0.04 \pm 0.06)\%$  for the O-AFE and IC-AFE cells in PLZT.

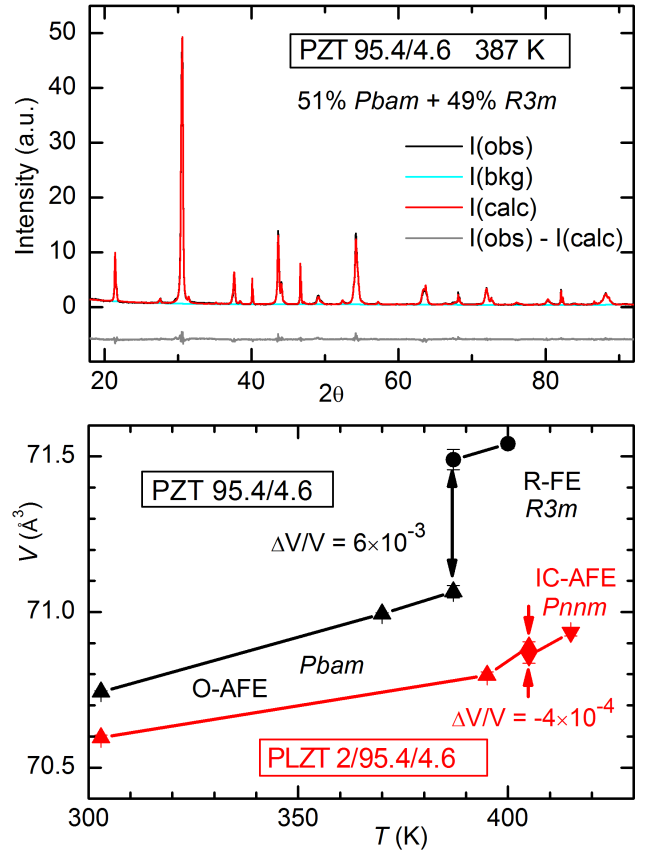


FIG. 7. Volumes of the pseudocubic unit cells R-FE ( $R3m$ ), O-AFE ( $Pbam$ ) and IC-AFE ( $Pnmm$ ) of PZT and PLZT around  $T_{AF}$ . In the upper panel is the refinement of the spectrum of PZT at  $T_{AF}$  with 51%  $Pbam$  + 49%  $R3m$ .

In addition,  $\text{La}^{3+}$  on the  $\text{Pb}^{2+}$  site, accompanied by Pb vacancies for charge compensation, is thought to destabilize the long range FE order<sup>25</sup>, because it introduces charge disorder and lacks the lone-pair that drives  $\text{Pb}^{2+}$  off-center. In the phase diagram of Asada and Koyama<sup>14</sup>, which constitutes the  $(x = 0.05) - y - T$  section in Fig. 5, the FE phase is found to be incommensurate, due to the concurrence of the AFE modes of Pb and of octahedral tilting. Note that also in La-free PZT with  $y(\text{Ti}) < 0.15$  the R-FE phase undergoes a phase transition below  $T_{IT}$ ,

which is evident in the compliance and therefore identified with non-polar short-range ordered (SRO) tilting of the octahedra<sup>23</sup>. The volume effect and the FE destabilization result in a rise of  $T_{AF}$  with  $x$  (La) and change of the intermediate phase from R-FE to IC-AFE.

That the nature of the intermediate phase below  $T_C$  is changed by 2% La doping is evident in the associated elastic anomaly (Fig. 4). In undoped PZT, when cooling from the PE phase one finds a very extended precursor softening ending in a spike at  $T_C$  and the compliance remains larger (or the modulus softer) in the FE phase. The softening in the FE phase is of piezoelectric origin<sup>22</sup>, and is therefore absent in the AFE phase. In fact, in Fig. 4 the  $s'$  curves of PZT and PLZT are very similar to each other, except for the lack of a higher plateau in the intermediate phase of PLZT.

More striking is the difference in the behaviors of the compliance during aging for the two compositions, illustrated in Figs. 2 and 6. The compliance of PZT at room temperature spans a range of nearly 400% of the stiffer value in the virgin state, exceptional for a ceramic, while PLZT remains stable within  $\pm 0.3\%$  after passing a larger number of cycles and 14 times longer aging.

The comparison between the two samples demonstrates that the elastic aging and fatigue in undoped PZT, the latter realized by the thermally induced transitions, are not simply related to the O-AFE phase, which is common to the two compositions, but are due to its coexistence with the FE phase. As a consequence, aging and fatigue must be connected to defects forming at the FE/AFE interfaces. The difference in volume between AFE and FE phases is the core of the explanations proposed for various aging and irreversible effects observed in diffraction and dielectric measurements of PZT-based materials<sup>9,24</sup>. The accommodation of the misfit strain has been proposed to cause broken and dangling bonds<sup>9</sup> and to promote the migration of the larger  $Zr^{4+}$  cations to the AFE domains and smaller  $Ti^{4+}$  and  $La^{3+}$  cations to the FE domains<sup>24</sup>. Also microcracking can be found in fatigued FE and AFE ceramics<sup>26,27</sup>, but neither microcracking nor a large/small cation imbalance should be the cause of the elastic aging discussed here, because they are not expected to be recovered by mild annealing well below the sintering temperature. In fact, the strong electric and elastic fields that might possibly promote the cation migration during the coexistence of the AFE and FE domains are missing in the C-PE phase, and under such conditions the cation migration occurs only at the sintering temperature. Also the similar observation of partial recovery of electrically fatigued PLZST after heating at  $\sim 770$  K for 1 h has been discussed in terms of migration of  $V_O$  or other charged species, rather than microcrack healing<sup>27</sup>.

The total cancelation of elastic aging and fatigue with 2% La doping is likely the result of multiple mechanisms. First of all, the FE phase becomes IC-AFE, whose smaller volume is closer to that of the O-AFE phase, and therefore reduces the misfit between the coexisting

phases when passing through the transition and aging within its region of thermal hysteresis. In addition to relieving the mechanical stresses, the substitution of the R-FE phase with IC-AFE, eliminates the electric fields at the borders of the FE domains, where the polarization charge is distributed<sup>28</sup>. Both the stress and electric fields would drive mobile defects like O vacancies<sup>29</sup> ( $V_O$ ), which possess different charge and specific volume with respect to  $O^{2-}$ . Though we do not have a quantitative model, we think that the main mechanism behind the elastic aging and fatigue effects is the migration of  $V_O$  to the charged and stressed walls between AFE and FE phases, followed by aggregation into relatively stable structures. Concentrations of few tenths of percent of  $V_O$  are always present as a result of the PbO loss during sintering, and their hypothetical linear or planar aggregations would certainly dissolve during moderate annealing. Note that the annealings in Fig. 2 are made in a vacuum of  $< 10^{-5}$  mbar, and therefore cannot fill  $V_O$ , but simply dissolve their aggregations. It is not obvious, however, how aggregations of small concentrations of  $V_O$ , likely well below 1%, would be able to soften the overall Young's modulus as much as observed. This remains an important point to be investigated, possibly with TEM and related techniques able to detect defect structures at the atomic level<sup>30</sup>.

As an additional mechanism, that contributes to preventing aging and fatigue in the La-doped material, one should consider the reduction or neutralization of the mobile defects. In fact,  $La^{3+}$  substituting  $Pb^{2+}$  is a donor, and makes the material electrically soft by improving the domain wall mobility, a phenomenon not well understood<sup>31</sup> but implicitly attributed to a reduction of the concentration of  $V_O$  that pin the domains.

In principle, the hopping of  $V_O$  should produce anelastic relaxation with one or more relaxation rates  $\tau^{-1}$ , detectable as one or more peaks in the  $Q^{-1}$  at the temperatures  $T_m$  and frequencies  $\omega/2\pi$  satisfying  $\omega\tau(T_m) \simeq 1$ <sup>21</sup>, as found in  $SrTiO_3$ <sup>32</sup>. Yet, already the apparently simple case of cubic  $SrTiO_3$  presents a complicated anelastic spectrum, due to isolated and variously aggregated  $V_O$ , with activation energies spanning from 0.6 to 1 eV; PLZT has the additional complication of strong traps, like Pb vacancies, and other perturbations like  $La^{3+}$  substituting  $Pb^{2+}$ . Moreover,  $Q^{-1}$  maxima from relaxation processes with activation energies  $E < 0.9$  eV are expected to appear at  $T_m < 500$  K, assuming  $\tau = \tau_0 \exp(E/T)$  with  $\tau_0 \sim 10^{-13}$  s and  $f \sim 2$  kHz, and would be masked by the losses associated with the domain wall motion below  $T_C$ . Indeed, we always observe at least two thermally activated  $Q^{-1}(T)$  peaks in the cubic phase of Zr-rich PZT, indicated as P1 and P2 in Fig. 8, and at least P1 at lower temperature may be due to hopping of  $V_O$ , though not simply isolated  $V_O$  in a regular lattice as in  $SrTiO_3$ . In fact, the high apparent activation energy, deduced from the shift of the peak in temperature when frequency changes, indicates correlated motions, similarly to the processes described by the Vogel-Fulcher law  $\tau = \tau_0 \exp E/(T - T_0)$ , where the slope of  $\ln \tau$  vs  $1/T$



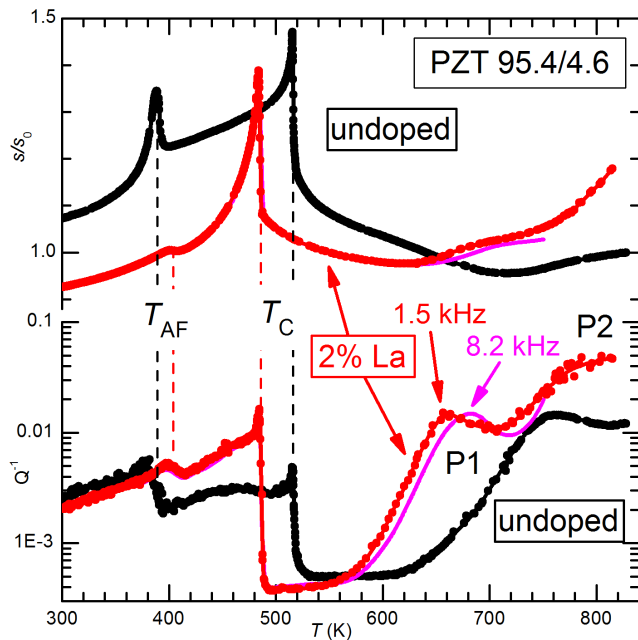


FIG. 8. Anelastic spectra of undoped and 2% La doped PZT 95.4/4.6 extended to high temperature. Of the doped sample are shown the curves measured during the same run at  $\sim 1.5$  and  $\sim 8.2$  kHz; the curves coincide except for the thermally activated relaxation processes P1 and P2.

exceeds  $E$  on approaching  $T_0$ . The high temperature anelastic spectra of the two samples are shown in Fig. 8 and, without attempting interpretations of the nature of the thermally activated peaks P1 and P2, we can say that they are due to mobile defects and P1 is most likely due to  $V_O$ , because the cations should not be able to perform  $10^4$  jumps per second below 700 K. Lanthanum doping does not suppress the heights of these peaks, but only shifts them to lower temperature, implying that about the same concentrations of defects is present, but with higher mobility. This observation seems to rule out a suppression of  $V_O$  by La doping, at least in this case.

## V. CONCLUSIONS

It is usually found that the AFE materials withstand repetitive electric cycling better than the FE materials<sup>26,33</sup> with some compositions withstanding  $10^7$  cycles before appreciable decrease in the saturation polarization and strain. Yet, the Young's modulus of AFE PZT may suffer huge softenings, up to a factor of 1/4, simply upon aging at room temperature few weeks with few thermally induced AFE/FE transitions. Though the temperature induced AFE/FE transition are different from the field induced ones, which are thought to involve only strain-free  $180^\circ$  switching, the magnitude of the presently reported phenomena suggests that materials for applications based on AFE/FE transitions, especially when induced by temperature changes, should be elastically tested also over long aging periods.

Doping with 2% La transforms the intermediate FE phase into IC-AFE, and completely suppresses the elastic aging: the Young's modulus is stable within  $\pm 0.3\%$  over more than one year and several thermal cycles.

It is proposed that the migration of O vacancies under the electric and stress fields at the AFE/FE interfaces and their aggregation into stable structures play a role in the elastic aging, since rapid annealing in vacuum at 800 K is sufficient to completely recover the original stiffness.

The awareness of so large a dependence of the elastic moduli on the sample history and of the presence of recoverable extended defects should be important when studying the methods for limiting the crack formation and propagation in these materials<sup>34,35</sup>.

## ACKNOWLEDGMENTS

The authors thank C. Capiani (ISTEC) for the preparation of the samples, Chiara Zanelli (ISTEC) for collecting the XRD spectra, and P. M. Latino (ISC) for his valuable technical assistance.

\* francesco.cordero@isc.cnr.it

<sup>1</sup> X. Hao, J. Zhai, L. B. Kong, and Z. Xu, *Progr. Mater. Sci.* **63**, 1 (2014).

<sup>2</sup> X. Tan, C. Ma, J. Frederick, S. Beckman, and K. G. Weber, *J. Am. Ceram. Soc.* **94**, 4091 (2011).

<sup>3</sup> X. Hao, Y. Zhao, and Q. Zhang, *J. Phys. Chem. C* **119**, 18877 (2015).

<sup>4</sup> A. S. Mischenko, Q. Zhang, J. F. Scott, R. W. Whatmore, and N. D. Mathur, *Science* **311**, 1270 (2006).

<sup>5</sup> X. Hao, Z. Yue, J. Xu, S. An, and C. W. Nan, *J. Appl. Phys.* **110**, 064109 (2011).

<sup>6</sup> S. Fähler, U. K. Rößler, O. Kastner, J. Eckert, G. Eggeler, H. Emmerich, P. Entel, S. Müller, E. Quandt, and K. Albe, *Adv. Eng. Mater.* **14**, 10 (2012).

<sup>7</sup> I. Takeuchi and K. Sandeman, *Physics Today* **68**, 48

(2015).

<sup>8</sup> X. Moya, S. Kar-Narayan, and N. D. Mathur, *Nat. Mater.* **13**, 439 (2014).

<sup>9</sup> B. P. Pokharel and D. Pandey, *J. Appl. Phys.* **86**, 3327 (1999).

<sup>10</sup> F. Cordero, F. Craciun, F. Trequattrini, C. Galassi, P. A. Thomas, D. S. Keeble, and A. M. Glazer, *Phys. Rev. B* **88**, 094107 (2013).

<sup>11</sup> F. Cordero, F. Trequattrini, F. Craciun, and C. Galassi, *Phys. Rev. B* **89**, 214102 (2014).

<sup>12</sup> In Refs. 10 and 11 we identified the stiffening on cooling with the orthorhombic tilt mode (OT) and the softening with the antiferroelectric mode (AF). At that time, as only explanation for a steplike stiffening during cooling through a structural phase transition we found the loss of one tilt

- system from the disordered tilted phase (with octahedral rotations about all axes) to the orthorhombic phase, un-tilted along the  $c$  axis. Now we are convinced of the importance of the piezoelectric softening in the FE phase, and therefore attribute the stiffening on cooling to the AF mode and the softening to the OT mode. What is written in Refs. 10 and 11 is valid if one exchanges AF with OT everywhere, except for some inessential comments to few fittings. Some of the fits of the  $s'(T)$  curves are slightly different, due to the compatibility conditions between the different phases embedded in the fitting equations, but the parameters remain identical or very similar with AF and OT exchanged. Also the discussion of the effect of the loss of tilting about the  $c$  axis remains valid, though evidently it is not enough to transform into stiffening the expected softening at the onset of the long range order below  $T_{OT}$ .
- <sup>13</sup> X. Dai, Z. Xu, and D. Viehland, *J. Appl. Phys.* **77**, 5086 (1995).
  - <sup>14</sup> T. Asada and Y. Koyama, *Phys. Rev. B* **69**, 104108 (2004).
  - <sup>15</sup> F. Cordero, F. Craciun, and C. Galassi, *Phys. Rev. Lett.* **98**, 255701 (2007).
  - <sup>16</sup> F. Cordero, F. Trequattrini, F. Craciun, and C. Galassi, *J. Phys.: Condens. Matter* **23**, 415901 (2011).
  - <sup>17</sup> D. L. Corker, A. M. Glazer, J. Dec, K. Roleder, and R. W. Whatmore, *Acta Cryst. B* **53**, 135 (1997).
  - <sup>18</sup> H. Liu and H. Toraya, *Jpn. J. Appl. Phys.* **38**, 104 (1999).
  - <sup>19</sup> C. Michel, J. M. Moreau, G. D. Achenbach, R. Gerson, and W. J. James, *Solid State Commun.* **7**, 865 (1969).
  - <sup>20</sup> F. Cordero, L. D. Bella, F. Corvasce, P. M. Latino, and A. Morbidini, *Meas. Sci. Technol.* **20**, 015702 (2009).
  - <sup>21</sup> A. S. Nowick and B. S. Berry, *Anelastic Relaxation in Crystalline Solids* (Academic Press, New York, 1972).
  - <sup>22</sup> F. Cordero, F. Craciun, F. Trequattrini, and C. Galassi, arXiv:1602.02799 (2016).
  - <sup>23</sup> F. Cordero, F. Trequattrini, F. Craciun, and C. Galassi, *Phys. Rev. B* **87**, 094108 (2013).
  - <sup>24</sup> V. M. Ishchuk and V. L. Sobolev, *J. Surf. Interf. Mater.* **3**, 35 (2015).
  - <sup>25</sup> X. Dai and D. Viehland, *J. Appl. Phys.* **76**, 3701 (1994).
  - <sup>26</sup> Q. Y. Jiang, E. C. Subbarao, and L. E. Cross, *J. Appl. Phys.* **75**, 7433 (1994).
  - <sup>27</sup> L. Zhou, A. Zimmermann, Y. P. Zeng, and F. Aldinger, *J. Am. Ceram. Soc.* **87**, 1591 (2004).
  - <sup>28</sup> Y. A. Genenko, *Phys. Rev. B* **78**, 214103 (2008).
  - <sup>29</sup> Y. A. Genenko and D. C. Lupascu, *Phys. Rev. B* **75**, 184107 (2007).
  - <sup>30</sup> D. I. Woodward, I. M. Reaney, G. Y. Yang, E. C. Dickey, and C. A. Randall, *Appl. Phys. Lett.* **84**, 4650 (2004).
  - <sup>31</sup> D. Damjanovic, *Rep. Prog. Phys.* **61**, 1267 (1998).
  - <sup>32</sup> F. Cordero, *Phys. Rev. B* **76**, 172106 (2007).
  - <sup>33</sup> L. Zhou, R. Z. Zuo, G. Rixecker, A. Zimmermann, T. Utschig, and F. Aldinger, *J. Appl. Phys.* **99**, 044102 (2006).
  - <sup>34</sup> K. Uchino, *Acta Mater.* **46**, 3745 (1998).
  - <sup>35</sup> X. Tan, S. E. Young, Y. H. Seo, J. Y. Zhang, W. Hong, and K. G. Webber, *Acta Mater.* **62**, 114 (2014).